

# Safe Robust Predictive Control-based Motion Planning of Automated Surface Vessels in Inland Waterways

Sajad Ahmadi\* Hossein Nejatbakhsh Esfahani\*  
Javad Mohammadpour Velni\*

\* Dept. of Mechanical Engineering, Clemson University, Clemson, SC  
29634 USA (e-mail: {sahmadi, hnejatb, javadm}@clemson.edu).

**Abstract:** Deploying self-navigating surface vessels in inland waterways offers a sustainable alternative to reduce road traffic congestion and emissions. However, navigating confined waterways presents unique challenges, including narrow channels, higher traffic density, and hydrodynamic disturbances. Existing methods for autonomous vessel navigation often lack the robustness or precision required for such environments. This paper presents a new motion planning approach for Automated Surface Vessels (ASVs) using Robust Model Predictive Control (RMPC) combined with Control Barrier Functions (CBFs). By incorporating channel borders and obstacles as safety constraints within the control design framework, the proposed method ensures both collision avoidance and robust navigation on complex waterways. Simulation results demonstrate the efficacy of the proposed method in safely guiding ASVs under realistic conditions, highlighting its improved safety and adaptability compared to the state-of-the-art.

**Keywords:** Autonomous Surface Vessels, Safety-Critical MPC, Control Barrier Functions, Inland Waterway Transportation.

## 1. INTRODUCTION

Inland water transportation (IWT) offers a sustainable solution to road congestion and the reduction of greenhouse gas emissions. Compared to road systems, waterways significantly lower transportation's environmental footprint (Bläsing et al., 2016). This potential, coupled with urbanization and logistics demands, has spurred interest in Automated Surface Vessels (ASVs) in IWT. ASVs promise safer and more efficient water transport by eliminating human errors and optimizing routes. However, integrating autonomous navigation technologies into IWT poses unique challenges due to confined waterways' narrow channels, high traffic density, and hydrodynamic phenomena. These constraints require specialized sensing and control algorithms for safe and efficient navigation, especially during overtaking or sharp turns Cheng et al. (2021).

A vision-based obstacle avoidance method for ASV navigation was proposed in Kim et al. (2019); however, its performance is highly sensitive to environmental conditions, and its ability to detect faraway objects is limited. To improve localization, Dhariwal and Sukhatme (2007) introduced a multi-sensor fusion approach that enhances the accuracy of the boat's position estimate. Meanwhile, dedicated efforts have been made in ASV trajectory planning Bitar et al. (2020) and trajectory tracking control Wang et al. (2016), yet these methods do not fully tackle the robust safety challenges inherent in dynamic, confined maritime environments.

Model Predictive Control (MPC) has gained widespread adoption for collision avoidance due to its ability to systematically handle both input and state constraints (Rawlings et al., 2017). In MPC, safety is typically enforced by incorporating constraints within the optimization problem. However, scenario-based MPC formulations—such as those employing dynamic probabilistic risk assessment (Trym et al., 2020) or incorporating COLREGs (Johansen et al., 2016)—often depend on the accuracy of state estimates and collision risk metrics, leaving them vulnerable under uncertainty. Other approaches, including tube-based MPC with LPV models (Yang et al., 2023) and dynamic programming-based robust control (Nejatbakhsh Esfahani and Szlapczynski, 2021), further underscore the challenges of achieving robust, computationally efficient ASV control.

Recent work in nonlinear robust MPC (Diehl et al., 2010; Lucia et al., 2012) and sample-based disturbance handling (Hewing and Zeilinger, 2019; Carvalho et al., 2014) illustrates the potential for advanced optimization techniques to manage uncertainties. Nonetheless, a critical gap remains in explicitly integrating safety constraints into these frameworks for the unique challenges of ASV navigation in confined waterways—a gap that the proposed RMPC-CBF framework seeks to address.

To the best of the authors' knowledge, no work on ASV navigation in confined waterways has carefully considered safety issues when obstacle avoidance and safe navigation are combined through narrow channels. As shown in Fig. 1, when navigating through a confined channel, ASVs should normally overtake on the port side, while the vessel

\* This work was supported by the US National Science Foundation under award CNS-2302215.

being overtaken should ideally be positioned as closely as possible to the starboard side of the channel.

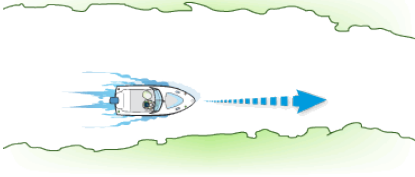


Fig. 1. ASVs navigating confined waterways must maintain safe clearance from channel borders.

This paper introduces a new RMPC-CBF framework for safe motion planning of Automated Surface Vessels (ASVs) in confined waterways, addressing the unique challenges posed by narrow channels and high traffic densities. By embedding the channel borders as Control Barrier Functions within the RMPC formulation, our approach effectively maintains safe distances while enabling dynamic maneuvers such as overtaking. This integrated method not only enhances collision avoidance and trajectory tracking under challenging hydrodynamic conditions but also achieves a critical balance between safety and performance, thereby advancing the state-of-the-art in ASV navigation.

Using CBFs has become popular for synthesizing safety-critical controllers due to their generality and relative ease of synthesis and implementation (Ames et al., 2017). Previous studies have explored the inclusion of safety considerations within the MPC framework to ensure that the controlled system operates within predefined safety boundaries. For example, barrier functions were utilized to develop a safety-critical MPC with CBFs by (Zeng et al., 2021), (Nejabatkhsh Esfahani et al., 2024) and (Nejabatkhsh Esfahani and Mohammadpour Velni, 2024).

The paper is organized as follows: Section 2 introduces the dynamic model of the ASV. Section 3 reviews CBFs in continuous and discrete time, setting the stage for our approach. Section 4 details the novel RMPC-CBF framework for safe motion planning in confined waterways. Section 5 presents simulation results demonstrating the framework's effectiveness and performance. Section 6 concludes with outcomes and future research directions.

## 2. MODELING OF AUTONOMOUS SURFACE VESSELS

In this paper, we adopt a 3-DOF model of a CyberShip (Skjetne et al., 2004). The dynamic is nonlinear and can be described in two reference frames: the body-fixed frame  $O_B$  and the Earth-fixed frame  $O_E$ , as shown in Fig. 2. The pose vector  $\boldsymbol{\eta} = [x, y, \psi]^T \in \mathbb{R}^3$  is in the Earth-fixed frame, where  $x$  is the North position,  $y$  is the East position and  $\psi$  is the heading angle. The velocity vector  $\boldsymbol{\nu} = [u, v, r]^T \in \mathbb{R}^3$  includes the surge  $u$  and sway  $v$  velocities and yaw rate  $r$  in the body-fixed frame. The control inputs and the external time-varying disturbances are labeled as  $\boldsymbol{\tau}, \boldsymbol{\tau}_d \in \mathbb{R}^3$ , respectively. The model can be represented as

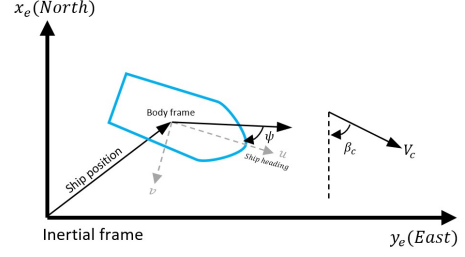


Fig. 2. Earth-fixed positioning and body-fixed motion frames for ASV surge, sway, and yaw.

$$\dot{\boldsymbol{\eta}} = J(\boldsymbol{\eta}) \boldsymbol{\nu}, \quad (1a)$$

$$M_{RB} \dot{\boldsymbol{\nu}} + M_A \dot{\boldsymbol{\nu}} + C_{RB}(\boldsymbol{\nu}) \boldsymbol{\nu} + C_A(\boldsymbol{\nu}) \boldsymbol{\nu} + D(\boldsymbol{\nu}) \boldsymbol{\nu} = \boldsymbol{\tau} + \boldsymbol{\tau}_d, \quad (1b)$$

where the rotation matrix  $J(\boldsymbol{\eta})$  is defined as

$$J(\boldsymbol{\eta}) = \begin{bmatrix} \cos(\psi) & -\sin(\psi) & 0 \\ \sin(\psi) & \cos(\psi) & 0 \\ 0 & 0 & 1 \end{bmatrix}. \quad (2)$$

The rigid-body inertia matrix  $M_{RB}$  and the added mass  $M_A$  are computed as

$$M_{RB} = \begin{bmatrix} m & 0 & 0 \\ 0 & m & mx_g \\ 0 & mx_g & I_z \end{bmatrix}, \quad M_A = \begin{bmatrix} -X_{\dot{u}} & 0 & 0 \\ 0 & -Y_{\dot{v}} & -Y_{\dot{r}} \\ 0 & -N_{\dot{v}} & -N_{\dot{r}} \end{bmatrix}, \quad (3)$$

where  $m$  is the mass of the ASV,  $I_z$  is the moment of inertia about the body  $z_b$ -axis (yaw axis), and  $x_g$  is the distance between the center of gravity and the body  $x_b$ -axis. Also, the rigid body and hydrodynamic of the Centripetal and Coriolis acceleration matrices are specified as

$$C_{RB}(\boldsymbol{\nu}) = \begin{bmatrix} 0 & 0 & -m(x_g r + v) \\ 0 & 0 & mu \\ m(x_g r + v) & -mu & 0 \end{bmatrix}, \quad (4)$$

$$C_A(\boldsymbol{\nu}) = \begin{bmatrix} 0 & 0 & c_{13} \\ 0 & 0 & c_{23} \\ -c_{13} & -c_{23} & 0 \end{bmatrix}, \quad (5)$$

with  $c_{13} = Y_{\dot{v}} v_r + 0.5(N_{\dot{v}} + Y_{\dot{r}})r$ ,  $c_{23} = -X_{\dot{u}} u_r$ , and  $X_{\dot{u}}, Y_{\dot{v}}, Y_{\dot{r}}, N_{\dot{v}}$  and  $N_{\dot{r}}$  are constant model parameters, while  $u_r$  and  $v_r$  are the reference frame surge and sway velocities, respectively. Moreover, the damping matrix reads as

$$D(\boldsymbol{\nu}) = \begin{bmatrix} d_{11} & 0 & 0 \\ 0 & d_{22} & d_{23} \\ 0 & d_{32} & d_{33} \end{bmatrix}, \quad (6)$$

where

$$d_{11} = X_u + X_{|u|u}|u| + X_{uuu}u_r^2, \quad (7a)$$

$$d_{22} = Y_v + Y_{|v|v}|v_r| + Y_{|r|r}|r|, \quad (7b)$$

$$d_{23} = Y_r + Y_{|v|r}|v_r| + Y_{|r|r}|r|, \quad (7c)$$

$$d_{32} = N_v + N_{|v|v}|v_r| + N_{|r|r}|r|, \quad (7d)$$

$$d_{33} = N_r + N_{|v|r}|v_r| + N_{|r|r}|r|, \quad (7e)$$

where the hydrodynamic coefficients are specified by  $X_{(\cdot)}, Y_{(\cdot)}$  and  $N_{(\cdot)}$ . Also,  $\boldsymbol{\tau} = [X, Y, N]^T$  includes the external control forces  $X, Y$  and the moment vector  $N$ . The thrusters are located in the back and the side of the ship, as depicted in Fig. 3. The actuator forces/torque

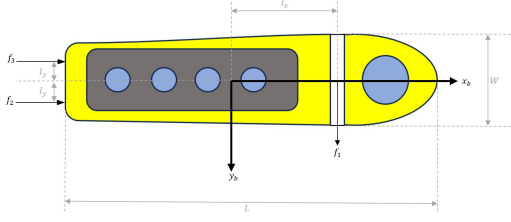


Fig. 3. Illustration of the ASV's rear and side thrusters, showing their placement for generating control forces and torque in confined waterway navigation.

vector is  $\mathbf{F} = [f_1, f_2, f_3]^\top$ , and the control input and the external disturbance vector are obtained as

$$\boldsymbol{\tau} = \mathbf{B}_T \mathbf{F}, \quad (8a)$$

$$\boldsymbol{\tau}_d = \mathbf{B}_T \boldsymbol{\omega}_d, \quad (8b)$$

where  $\boldsymbol{\omega}_d \in \mathbb{R}^3$  is the disturbance vector. The thruster allocation matrix is given by

$$\mathbf{B}_T = \begin{bmatrix} 0 & 0 & 1 \\ 1 & 0 & 0 \\ l_x & -l_y & l_y \end{bmatrix}, \quad (9)$$

with  $l_x$  and  $l_y$  denoting the offsets from the vessel's center of gravity to the thrusters in the longitudinal and lateral directions, respectively (see Fig. 3). This configuration ensures that the spatial arrangement of the thrusters is accurately incorporated into the resulting control input.

### 3. REVIEW OF CONTROL BARRIER FUNCTIONS

Control barrier functions (CBFs) have been proposed to ensure safety in safety-critical systems by restricting the control inputs to an acceptable range. This is achieved by defining safety requirements as the need for a system to remain within a defined safe set. To accomplish this, we define a set  $\mathcal{C}$  as the region above a continuously differentiable function  $h : \mathcal{D} \subset \mathbb{R}^n \rightarrow \mathbb{R}$ , where  $\mathcal{D}$  represents a subset of  $n$ -dimensional real numbers such that

$$\begin{aligned} \mathcal{C} &= \{\mathbf{x} \in \mathcal{D} \subset \mathbb{R}^n : h(\mathbf{x}) \geq 0\}, \\ \partial\mathcal{C} &= \{\mathbf{x} \in \mathcal{D} \subset \mathbb{R}^n : h(\mathbf{x}) = 0\}, \\ \text{Int}(\mathcal{C}) &= \{\mathbf{x} \in \mathcal{D} \subset \mathbb{R}^n : h(\mathbf{x}) > 0\}, \end{aligned} \quad (10)$$

where  $\partial\mathcal{C}$  and  $\text{Int}(\mathcal{C})$  are the boundary of  $\mathcal{C}$  and the interior of  $\mathcal{C}$ , respectively. In addition, we make the assumption that the interior of the set  $\mathcal{C}$  is not empty (denoted as  $\text{Int}(\mathcal{C}) \neq \emptyset$ ). We then define  $\mathcal{C}$  as the “safe set.” A CBF is considered successful in certifying forward invariance of  $\mathcal{C}$  if it ensures that the system trajectory remains inside the safe set and does not approach its boundary. Let us consider a nonlinear system in control-affine form as

$$\dot{\mathbf{x}} = \mathbf{f}(\mathbf{x}) + g(\mathbf{x}) \mathbf{u}, \quad (11)$$

where  $\mathbf{f} : \mathbb{R}^n \rightarrow \mathbb{R}^n$  and  $g : \mathbb{R}^n \rightarrow \mathbb{R}^{n \times m}$  are locally Lipschitz continuous functions,  $\mathbf{x} \in \mathbb{R}^n$  and  $\mathbf{u} \in \mathbb{R}^m$  are the system states and control inputs, respectively. The closed-loop dynamic of the system is then described as

$$\dot{\mathbf{x}} = \mathbf{f}_{\text{cl}}(\mathbf{x}) = \mathbf{f}(\mathbf{x}) + g(\mathbf{x}) \mathbf{u}|_{\boldsymbol{\pi}(\mathbf{x})}, \quad (12)$$

where the control policy (feedback controller)  $\boldsymbol{\pi} : \mathbb{R}^n \rightarrow \mathbb{R}^m$  is locally Lipschitz continuous. Consider a maximum interval of existence denoted as  $I(\mathbf{x}_0) = [t_0, t_{\max}]$  for any

initial condition  $\mathbf{x}_0$  in the subset  $\mathcal{D}$ . This interval ensures that the trajectory  $\mathbf{x}(t)$  represents the unique solution to (12) within the interval  $I(\mathbf{x}_0)$ . If  $t_{\max}$  is set to infinity, the closed-loop system  $\mathbf{f}_{\text{cl}}$  is considered forward complete, implying that the system's solutions can be extended indefinitely into the future.

*Definition 1.* (Ames et al., 2019) (Forward Invariance) The closed-loop system (12) is forward invariant w.r.t the set  $\mathcal{C}$  if for every  $\mathbf{x}_0 \in \mathcal{C}$ , we have  $\mathbf{x}(t) \in \mathcal{C}$  for all  $t \in I(\mathbf{x}_0)$ .

*Definition 2.* (Ames et al., 2019) (Control Barrier Function) Given a dynamical system (11) and the safe set  $\mathcal{C}$  with a continuously differentiable function  $h : \mathcal{D} \rightarrow \mathbb{R}$ , then  $h$  is a CBF if there exists a class  $\mathcal{K}_\infty$  function  $\kappa$  for all  $\mathbf{x} \in \mathcal{D}$  such that

$$\sup_{\mathbf{u} \in \mathcal{U}} \{L_f h(\mathbf{x}) + L_g h(\mathbf{x}) \mathbf{u}\} \geq -\kappa(h(\mathbf{x})), \quad (13)$$

where  $\dot{h}(\mathbf{x}, \mathbf{u}) = L_f h(\mathbf{x}) + L_g h(\mathbf{x}) \mathbf{u}$  with  $L_f h, L_g h$  as the Lie derivatives of  $h$  along the vector fields  $\mathbf{f}$  and  $g$ . A common choice for the function  $\kappa$  is a linear form given by  $\kappa(h(\mathbf{x})) = \alpha h(\mathbf{x})$ , where the parameter  $\alpha \geq 0$  influences the system behavior near the boundary of  $h(\mathbf{x}) = 0$ .

The above condition in discrete time becomes

$$\Delta h(\mathbf{x}_k) \geq -\gamma h(\mathbf{x}_k), \quad 0 < \gamma \leq 1, \quad (14)$$

where  $\Delta h(\mathbf{x}_k) := h(\mathbf{x}_{k+1}) - h(\mathbf{x}_k)$ .

### 4. SAFETY-CRITICAL CONTROL DESIGN

In this section, we first formulate the safety functions required in the discrete-time CBFs (14) to address a safe motion planning of ASVs in confined inland waterways. We then formulate the safety-critical RMPC scheme based on the proposed CBFs.

#### 4.1 Safety Functions

This paper addresses two types of unsafe zones formulated as discrete-time CBFs. The first type describes some obstacles  $i = 1, \dots, n_o$  for which the safety function  $h_i^o(x_k, y_k)$  is defined as

$$h_i^o(x_k, y_k) := -1 + \frac{\left((x_k - o_{x,i})^2 + (y_k - o_{y,i})^2\right)}{(r_i + r_a)^2} \geq 0, \quad (15)$$

where  $(o_{x,i}, o_{y,i})$  and  $r_i$  are the center and radius of the  $i^{\text{th}}$  obstacle, respectively. The constant  $r_a$  is the radius of the ASV. The second type of unsafe zone is considered for the borders of the inland waterway. To this end, we define these borders by two straight lines  $L_j$ , where  $j = 1, 2$ . Each line is then characterized by

$$L_j := a_j x_k + b_j y_k + c_j = 0, \quad j = 1, \dots, z \quad (16)$$

where  $z$  is the number of border lines and  $a_{\ell,j}, b_{\ell,j}, c_{\ell,j} \in \mathbb{R}$  are the parameters of each line. The corresponding safe set is then obtained as

$$\mathcal{C}_b = \{\mathbf{P}_k \in \mathbb{R}^2 | L_1 \geq 0 \cap L_2 \geq 0\}, \quad (17)$$

where  $\mathbf{P}_k = [x_k, y_k]^\top$  is the 2D position vector of the ASV. Let us define the distance between the ASV and each waterway border as

$$D_j(\mathbf{P}_k) = \frac{a_j x_k + b_j y_k + c_j}{\sqrt{a_j^2 + b_j^2}}. \quad (18)$$

The safety functions  $h_j^b(\mathbf{P}_k)$  used in the corresponding CBFs are then defined by

$$h_j^b(\mathbf{P}_k) := D_j(\mathbf{P}_k) - \frac{\sqrt{w^2 + l^2}}{2}, \quad (19)$$

where  $w$  and  $l$  denote the width and length of the ASV, respectively.

#### 4.2 Design of Robust Safety-Critical RMPC Scheme

Let  $\dot{\mathbf{x}} = \bar{\mathbf{f}}(\mathbf{x}, \mathbf{u}, \boldsymbol{\omega}^r)$  be the continuous-time, state-space description of the ASV, where  $\mathbf{x} = [\boldsymbol{\eta}, \boldsymbol{\nu}]^\top$  and  $\boldsymbol{\omega}^r \in \mathbb{R}^3$  is the disturbance applied to the real system. The discretized model then reads  $\mathbf{x}_{k+1} = \mathbf{f}(\mathbf{x}_k, \mathbf{u}_k, \boldsymbol{\omega}_k^r)$ . We assume that a full measurement or estimate of the state vector  $\mathbf{x}_k$  is available at the current time instant  $k$ . We then design our safety-critical controller, addressing the motion planning of ASVs while ensuring safety issues in inland waterways. The proposed safety-critical RMPC solves the following constrained finite-time Optimal Control Problem (OCP) with a prediction horizon of length  $N$  at each time instant  $k$ .

##### Proposed Robust MPC-CBF Problem:

$$J = \min_{\mathbf{x}, \mathbf{u}} \left\{ V(\mathbf{x}_N) + \max_{\boldsymbol{\omega}} \left\{ \sum_{k=0}^{N-1} L(\mathbf{x}_k, \mathbf{u}_k, \boldsymbol{\omega}_k) \right\} \right\} \quad (20a)$$

$$\text{s.t.} \quad (20b)$$

$$\mathbf{x}_{k+1} = \mathbf{f}(\mathbf{x}_k, \mathbf{u}_k, \boldsymbol{\omega}_k), \quad (20c)$$

$$\mathbf{g}(\mathbf{u}_k) \leq 0, \quad (20d)$$

$$\mathbf{q}(\mathbf{x}_k, \mathbf{u}_k) \leq 0, \quad \mathbf{q}_f(\mathbf{x}_N, \mathbf{u}_N) \leq 0, \quad (20e)$$

$$\boldsymbol{\omega}_{min} \leq \boldsymbol{\omega}_k \leq \boldsymbol{\omega}_{max}, \quad (20f)$$

$$\Delta h_i^o(\mathbf{x}_k) + \gamma_i^o h_i^o(\mathbf{x}_k) \geq 0, \quad i = 1, \dots, n_o, \quad (20g)$$

$$\Delta h_j^b(\mathbf{x}_k) + \gamma_j^b h_j^b(\mathbf{x}_k) \geq 0, \quad j = 1, 2. \quad (20g)$$

In (20a),  $V$  and  $L$  denote the terminal and stage costs, respectively. The control input constraints are introduced by  $\mathbf{g}(\mathbf{u}_k)$  while  $\mathbf{q}_f$  and  $\mathbf{q}$  are the mixed terminal and stage inequality constraints, respectively. The first element of the optimal control input sequence  $\mathbf{u}_{0, \dots, N-1}^*$  is then applied to the ASV, and the above OCP is solved at each time instant based on the latest state of the system. The disturbance vector  $\boldsymbol{\omega}_k = [\omega_x, \omega_y, 0]^\top$  is bounded as  $\underline{\omega}_x \leq \omega_x \leq \bar{\omega}_x$  and  $\underline{\omega}_y \leq \omega_y \leq \bar{\omega}_y$ , where  $\omega_x$  and  $\omega_y$  denote the disturbance in  $x$  and  $y$  directions, respectively. The constraints (20f) and (20g) denote the proposed CBF conditions on the obstacles  $1, \dots, n_o$  and borders  $1, 2$ , respectively, and are enforced at every time step within the prediction horizon. In this paper, we consider a quadratic form for  $V$  and  $L$  as described in the next section. The proposed approach aims to solve the robust model predictive control (RMPC) problem by minimizing the worst-case cost under bounded disturbances. Let the disturbance inputs  $\omega_x$  and  $\omega_y$  be quantized into  $N_\omega$  levels. At each time instant  $k$ , we select the disturbance value  $\omega_k$  that maximizes the stage cost function

$$\omega_k = \arg \max_{\omega \in \mathcal{W}} L(\mathbf{x}_k, \mathbf{u}_k, \omega_k), \quad (21)$$

where  $\mathcal{W}$  represents the set of all possible discrete disturbance values, defined as

$$\mathcal{W}_x = \{\omega_x^1, \omega_x^2, \dots, \omega_x^{N_\omega}\}, \quad \mathcal{W}_y = \{\omega_y^1, \omega_y^2, \dots, \omega_y^{N_\omega}\},$$

such that each  $\omega_x^{(\cdot)}$  and  $\omega_y^{(\cdot)}$  is a quantized level within the bounded range  $[\underline{\omega}_x, \bar{\omega}_x]$  and  $[\underline{\omega}_y, \bar{\omega}_y]$ , respectively. The overall disturbance set is then  $\mathcal{W} = \mathcal{W}_x \times \mathcal{W}_y$ . Then, we incorporate a conditional constraint for each quantized disturbance level, which forces the optimizer to select the disturbance level that results in the maximum stage cost  $L$  over  $\omega$ . Finally, the cost  $J$  will be minimized under the constraints. Algorithm 1 outlines the proposed approach in a more organized way.

##### Algorithm 1 Implementation of Robust MPC Scheme

```

1: Get initial position and final destination of the ASV
   ( $\mathbf{x}_0$  and  $\mathbf{x}_f$ )
2:  $J \leftarrow 0$ 
3:  $\text{tol} \leftarrow 0.3$ 
4: while  $\|\mathbf{x} - \mathbf{x}_f\|_2 \geq \text{tol}$  do
5:   for  $k = 0 \rightarrow N - 1$  do
6:      $\boldsymbol{\omega}_{\text{worst}}^k \leftarrow [0, 0]^\top$ 
7:      $L_{\text{max}}^k \leftarrow 0$ 
8:     for  $\omega_x \in \mathcal{W}_x$  do
9:       for  $\omega_y \in \mathcal{W}_y$  do
10:         $L^k(\mathbf{x}_k, \mathbf{u}_k) \leftarrow L(\mathbf{x}_k, \mathbf{u}_k, [\omega_x, \omega_y, 0])$ 
11:        if  $L^k(\mathbf{x}_k, \mathbf{u}_k) > L_{\text{max}}^k$  then
12:           $L_{\text{max}}^k \leftarrow L^k(\mathbf{x}_k, \mathbf{u}_k)$ 
13:           $\boldsymbol{\omega}_{\text{worst}}^k \leftarrow [\omega_x, \omega_y, 0]^\top$ 
14:        end if
15:      end for
16:    end for
17:     $J \leftarrow J + L_{\text{max}}^k$ 
18:  end for
19:   $J \leftarrow J + V(\mathbf{x}_N)$ 
20:  Solve the problem of minimizing cost  $J$  subject to
   (20b)-(20g) to find  $\mathbf{u}$  (20).
21:  Apply  $\mathbf{u}_0^*$  to real system  $\mathbf{x}_{k+1} = \mathbf{f}(\mathbf{x}_k, \mathbf{u}_k, \boldsymbol{\omega}_k^r)$ .
22: end while

```

**Remark 1:** We note that the main contribution of this work is in the application of RMPC-CBF algorithm in ASVs. A parallel work is exploring theoretical guarantees for the stability and recursive feasibility of the proposed predictive control scheme.

#### 5. SIMULATION RESULTS AND DISCUSSION

In this section, we examine the performance of the proposed safety-critical RMPC for ASV's motion planning. In this scenario, an ASV must safely navigate among static obstacles while avoiding the boundaries of the inland waterway and approaching the final destination. To examine the robustness of the proposed safety-critical RMPC, we consider some external disturbances induced by water flow. The water flow force in the channel is represented by the vector  $\mathbf{d}_f = \{f, \beta\}$ , where  $f$  is the flow force and  $\beta$  is the flow angle. In our simulations, the flow force  $f$  is generated as

$$f = \sqrt{\sin^2(x+y) + \sin^2(x-y)}, \quad (22)$$

and the flow angle  $\beta$  is defined as

$$\beta = \tan^{-1} \left( \frac{\sin(x-y)}{\sin(x+y)} \right), \quad (23)$$

where  $x$  and  $y$  are the first two states of the system, respectively. The disturbances acting on the ASV are

$\omega_x = f \cos(\beta)$  and  $\omega_y = f \sin(\beta)$ , which will be added to the control inputs  $f_{surge}$  and  $f_{sway}$ , respectively.

We select a sampling time of 0.2 sec. to discretize the continuous-time ASV model and set the prediction horizon to  $N = 10$ . The terminal and stage costs in the RMPC-CBF scheme (20) are defined as

$$V(\mathbf{x}_N) = (\mathbf{x}_N - \mathbf{r}_d)^\top Q_T (\mathbf{x}_N - \mathbf{r}_d), \quad (24)$$

$$L(\mathbf{x}_k, \mathbf{u}_k, \boldsymbol{\omega}_k) = \quad (25)$$

$$(\mathbf{x}_k - \mathbf{r}_d)^\top Q (\mathbf{x}_k - \mathbf{r}_d) + (\Delta \tilde{\mathbf{u}}_k)^\top R (\Delta \tilde{\mathbf{u}}_k)$$

where  $\mathbf{r}_d$  is the desired state vector,  $\Delta \tilde{\mathbf{u}}_k = \tilde{\mathbf{u}}_k - \tilde{\mathbf{u}}_{k-1}$ , and  $\tilde{\mathbf{u}}_k = \mathbf{u}_k - [\omega_{x,k}; \omega_{y,k}; 0]$ . The corresponding weights are then selected as  $Q_T = \text{diag}([3, 3, 3, 1, 1, 1])$ ,  $Q = \text{diag}([2, 2, 2, 1, 1, 1])$ ,  $R = \text{diag}([0.1, 0.1, 0.01])$ , and other parameters are  $N_\omega = 20$ ,  $w_{min} = -\sqrt{2}$ ,  $w_{max} = \sqrt{2}$ ,  $u_{min} = [-8, -8, -8]$ ,  $u_{max} = [8, 8, 8]$ .

To solve the RMPC optimization problem, we employed CasADi with IPOPT as the solver (Andersson et al., 2019). The motion planning scenario aims to safely guide the ASV from the initial position  $P_i = [0, 2, 0]$ , where it starts at rest, to the final destination  $P_f = [25, 3, 0]$ , where it comes to a complete stop.

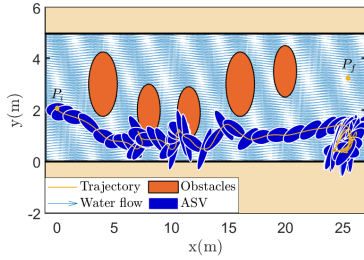


Fig. 4. The figure shows the ASV's trajectory with a non-robust MPC. Starting at  $P_i$ , the ASV struggles to navigate through the region, which includes water flows (blue arrows) and obstacles (orange shapes). ASV trajectory under non-robust MPC control shows collisions with obstacles and borders due to the inability to handle disturbances and maintain constraints.

Fig. 4 shows the ASV's trajectory when employing a conventional (non-robust) MPC scheme. Due to the influence of water flow disturbances (shown by blue arrows) and the presence of static obstacles (shown as orange shapes), the ASV struggles to follow a safe path. With the lack of robustness in disturbance handling, the ASV collides with both the obstacles and the channel boundaries, making this method unsuitable for safe navigation. In contrast, Fig. 5a demonstrates the effectiveness of the proposed RMPC-CBF framework. The ASV's trajectory, represented in green, successfully avoids obstacles while remaining within the channel boundaries. The incorporation of the CBFs ensures a collision-free navigation by imposing safety constraints on both obstacles and waterway borders. Additionally, Fig. 5b shows a close-up view of the ASV's trajectory, highlighting its ability to maneuver through the waterway without violating safety constraints.

Fig. 6 shows that while enforcing hard state constraints ensures that the ASV remains within the channel boundaries, this approach does not adjust for varying operational con-

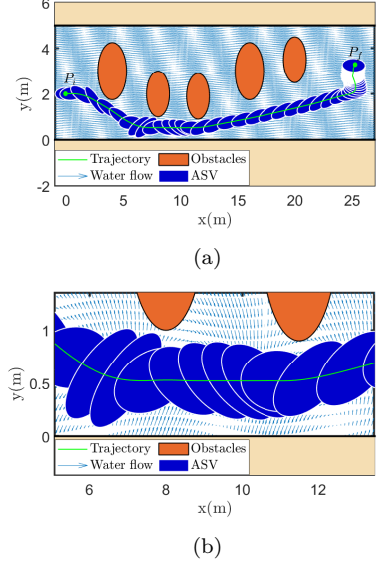


Fig. 5. (a) The green trajectory starts from  $P_i$ , showing safe navigation using the proposed safety critical RMPC when we have the CBF on the upper and lower borders and all the obstacles with  $\gamma^o = 0.15$  and  $\gamma^b = 0.9$ . The safe trajectory of the ASV under the proposed RMPC-CBF framework demonstrates successful obstacle and border avoidance in a confined waterway influenced by disturbances. (b) A zoomed view of the ASV's trajectory shows precise obstacle avoidance and safe navigation along the waterway borders using the proposed RMPC-CBF control.

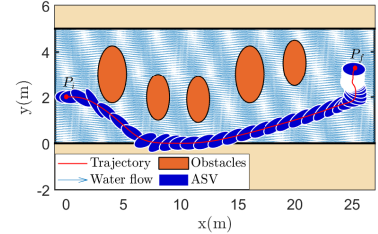


Fig. 6. ASV trajectory under robust MPC employing hard state constraints for border avoidance. While these constraints effectively prevent the vessel from exiting the channel, they do not offer the adaptive safety margins of the CBF-based approach, resulting in inadequate clearance from the borders during sharp turns and occasional contact with the channel boundaries.

ditions, resulting in insufficient clearance from the channel edges during sharp maneuvers.

Finally, Fig. 7a and 7b compare the speed and control inputs across different scenarios. The results indicate that the RMPC-CBF approach ensures smoother and safer transitions in velocity and control inputs while maintaining speed efficiency.

## 6. CONCLUSIONS

This paper presents a safety-critical control design approach for motion planning of an ASV in confined inland waterways. We used the CBF framework to design a safety-critical RMPC scheme for ASVs. To address safety issues, we formulated safety functions to avoid the border water-



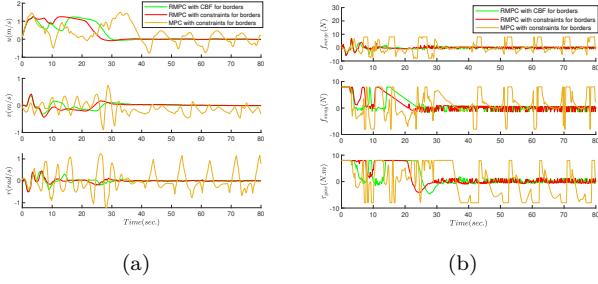


Fig. 7. (a) Comparison of ASV speeds under RMPC-CBF, RMPC with border constraints, and non-robust MPC. (b) Control inputs comparison for ASV navigation using RMPC-CBF, RMPC with border constraints, and non-robust MPC, demonstrating the smoother and more stable control achieved with RMPC.

way and obstacles. These functions defined discrete-time CBFs embedded in the RMPC formulation. We demonstrated the proposed method's performance compared to non-robust MPC and RMPC without CBF constraints.

Future work will investigate the theoretical guarantees, accelerating computation, and extending the scheme to cooperative multi-ASV navigation in dynamic environments to enable large-scale deployment. Furthermore, addressing dynamic obstacles and real-time changes will enhance adaptability and enable safe, large-scale ASV deployment.

## REFERENCES

- Ames, A.D., Coogan, S., Egerstedt, M., Notomista, G., Sreenath, K., and Tabuada, P. (2019). Control barrier functions: Theory and applications. In *2019 18th European control conference (ECC)*, 3420–3431. IEEE.
- Ames, A.D., Xu, X., Grizzle, J.W., and Tabuada, P. (2017). Control barrier function based quadratic programs for safety critical systems. *IEEE Transactions on Automatic Control*, 62(8), 3861–3876.
- Andersson, J.A., Gillis, J., Horn, G., Rawlings, J.B., and Diehl, M. (2019). Casadi: a software framework for nonlinear optimization and optimal control. *Mathematical Programming Computation*, 11, 1–36.
- Bitar, G., Martinsen, A.B., Lekkas, A.M., and Breivik, M. (2020). Two-stage optimized trajectory planning for ASVs under polygonal obstacle constraints: Theory and experiments. *IEEE Access*, 8, 199953–199969.
- Bläsing, M., Kistler, M., and Lehdorff, E. (2016). Emission fingerprint of inland navigation vessels compared with road traffic, domestic heating and ocean going vessels. *Organic geochemistry*, 99, 1–9.
- Carvalho, A., Gao, Y., Lefevre, S., and Borrelli, F. (2014). Stochastic predictive control of autonomous vehicles in uncertain environments. In *12th international symposium on advanced vehicle control*, volume 9.
- Cheng, Y., Jiang, M., Zhu, J., and Liu, Y. (2021). Are we ready for unmanned surface vehicles in inland waterways? the usvinland multisensor dataset and benchmark. *IEEE Robotics and Automation Letters*, 6(2), 3964–3970.
- Dhariwal, A. and Sukhatme, G.S. (2007). Experiments in robotic boat localization. In *2007 IEEE/RSJ International Conference on Intelligent Robots and Systems*, 1702–1708. IEEE.
- Diehl, M., Amrit, R., and Rawlings, J.B. (2010). A lyapunov function for economic optimizing model predictive control. *IEEE Transactions on Automatic Control*, 56(3), 703–707.
- Hewing, L. and Zeilinger, M.N. (2019). Scenario-based probabilistic reachable sets for recursively feasible stochastic model predictive control. *IEEE Control Systems Letters*, 4(2), 450–455.
- Johansen, T.A., Perez, T., and Cristofaro, A. (2016). Ship collision avoidance and COLREGS compliance using simulation-based control behavior selection with predictive hazard assessment. *IEEE transactions on intelligent transportation systems*, 17(12), 3407–3422.
- Kim, H., Koo, J., Kim, D., Park, B., Jo, Y., Myung, H., and Lee, D. (2019). Vision-based real-time obstacle segmentation algorithm for autonomous surface vehicle. *IEEE Access*, 7, 179420–179428.
- Lucia, S., Finkler, T., Basak, D., and Engell, S. (2012). A new robust nmpc scheme and its application to a semi-batch reactor example. *IFAC Proceedings Volumes*, 45(15), 69–74.
- Nejatbakhsh Esfahani, H., Ahmadi, S., and Mohammadpour Velni, J. (2024). Learning-based safety critical model predictive control using stochastic control barrier functions. In *2024 American Control Conference (ACC)*. IEEE.
- Nejatbakhsh Esfahani, H. and Mohammadpour Velni, J. (2024). Safe mpc-based motion planning of auvs using mhe-based approximate robust control barrier functions. In *2024 32nd Mediterranean Conference on Control and Automation (MED)*. IEEE.
- Nejatbakhsh Esfahani, H. and Szlapczynski, R. (2021). Robust-adaptive dynamic programming-based time-delay control of autonomous ships under stochastic disturbances using an actor-critic learning algorithm. *Journal of Marine Science and Technology*, 26, 1262–1279.
- Rawlings, J.B., Mayne, D.Q., and Diehl, M. (2017). *Model predictive control: theory, computation, and design*, volume 2. Nob Hill Publishing Madison, WI.
- Skjetne, R., Smogeli, Ø., and Fossen, T.I. (2004). Modeling, identification, and adaptive maneuvering of cybership ii: A complete design with experiments. *IFAC Proceedings Volumes*, 37(10), 203–208.
- Trym, T., Brekke, E.F., and Johansen, T.A. (2020). On collision risk assessment for autonomous ships using scenario-based MPC. *IFAC-PapersOnLine*, 53(2), 14509–14516.
- Wang, N., Lv, S., Er, M.J., and Chen, W.H. (2016). Fast and accurate trajectory tracking control of an autonomous surface vehicle with unmodeled dynamics and disturbances. *IEEE Transactions on Intelligent Vehicles*, 1(3), 230–243.
- Yang, H., Li, B., Zuo, Z., and Zhao, H. (2023). Tube-based MPC for LPV systems with external disturbances using interval predictors. *IEEE Transactions on Industrial Informatics*.
- Zeng, J., Zhang, B., and Sreenath, K. (2021). Safety-critical model predictive control with discrete-time control barrier function. In *2021 American Control Conference (ACC)*, 3882–3889. IEEE.